In vivo Molecular Imaging of Cancer with a Quenching Near-Infrared Fluorescent Probe Using Conjugates of Monoclonal Antibodies and Indocyanine Green

Mikako Ogawa, Nobuyuki Kosaka, Peter L. Choyke, and Hisataka Kobayashi

Molecular Imaging Program, Center for Cancer Research, National Cancer Institute/NIH, Bethesda, Maryland

Abstract

Near-infrared (NIR) fluorophores have several advantages over visible fluorophores, including improved tissue penetration and lower autofluorescence; however, only indocyanine green (ICG) is clinically approved. Its use in molecular imaging probes is limited because it loses its fluorescence after protein binding. This property can be harnessed to create an activatable NIR probe. After cell binding and internalization, ICG dissociates from the targeting antibody, thus activating fluorescence. ICG was conjugated to the antibodies daclizumab (Dac), trastuzumab (Tra), or panitumumab (Pan). The conjugates had almost no fluorescence in PBS but became fluorescent after SDS and 2-mercaptoethanol, with a quenching capacity of 10-fold for 1:1 conjugates and 40- to 50-fold for 1:5 conjugates. *In vitro* microscopy showed activation within the endolysosomes in target cells. *In vivo* imaging in mice showed that CD25-expressing tumors were specifically visualized with Dac-ICG. Furthermore, tumors overexpressing HER1 and HER2 were successfully characterized *in vivo* by using Pan-ICG(1:5) and Tra-ICG(1:5), respectively. Thus, we have developed an activatable NIR optical probe that "switches on" only in target cells. Because both the antibody and the fluorophore are Food and Drug Administration approved, the likelihood of clinical translation is improved. [Cancer Res 2009;69(4):1268–72]

Introduction

Molecular imaging probes that use near-infrared (NIR, emission spectra ~700–850 nm) fluorophores offer several advantages over visible fluorophores. NIR probes have better tissue penetration, less autofluorescence, and large Stokes shifts, allowing better rejection of excitation light (1, 2). Only indocyanine green (ICG), which has absorption at ~780 nm and emission at ~820 nm, has been approved by the Food and Drug Administration (FDA) and is in clinical use for over 30 years with an excellent safety record (3, 4). Unfortunately, the conjugation chemistry of ICG is difficult because of its amphophilicity and few functional groups. Although protein binding is possible, once bound to protein, ICG dramatically loses its fluorescence. That feature has dissuaded investigators from using ICG in molecular imaging probes. However, this property can be harnessed to create activatable NIR optical probes.

Activation of optical probes can be achieved using mechanisms including photon-induced electron transfer (5, 6), self-quenching (homo-FRET; ref. 7), and quencher-fluorophore interaction (hetero-FRET). Activation leads to high tumor-to-background ratios because unbound agents yield little signal. Once ICG conjugated with proteins, fluorescence is markedly decreased (8–10). However, upon catabolism, light is once again emitted.

A probe that targets cells and internalizes could lead to high tumor-to-background ratios if the probe activates upon internalization. By combining ICG with FDA-approved monoclonal antibodies (mAb) directed at cell surface markers overexpressed on cancers (anti-CD25, anti-EGFR1, and anti-HER2), we show the feasibility of using ICG-mAb conjugates as activatable *in vivo* molecular imaging probes. The possibilities of clinical translation are greatly enhanced because both components of this probe, the targeting moiety and the fluorophore, are already FDA approved.

Materials and Methods

Reagents. ICG-sulfo-OSu was purchased from Dojindo Molecular Technologies. The following mAbs were used: daclizumab (Dac), humanized mAb to the IL-2Rα (CD25; Hoffmann-La Roche, Inc.); panitumumab (Pan), human anti-HER1 IgG2 mAb (AMGEN, Inc.); trastuzumab (Tra), humanized anti–HER-2 mAb (Genentech, Inc.); and human polyclonal IgG, a control antibody (Sigma Chemical). ZsGreen plasmid was purchased from Clontech Laboratories, Inc. All other chemicals used were of reagent grade.

Synthesis of ICG-conjugated antibodies. Daclizumab (1 mg, 6.8 nmol) was incubated with ICG-sulfo-OSu (6.8 or 68 nmol) in 0.1 mol/L Na_2HPO_4 (pH 8.5) at room temperature for 30 min. The mixture was purified with a Sephadex G50 column (PD-10; GE Healthcare). The protein concentration was determined with CoomassiePlus protein assay kit (Pierce Biotechnology). The concentration of ICG was measured by absorption with the UV-Vis system to confirm numbers of fluorophore molecules conjugated to each trastuzumab molecule. The absorption was also measured in 5% SDS and 2-mercaptoethanol (2-ME), which were added to diminish hydrophobic interaction among ICG molecules and between ICG and the antibody. For HER1 or HER2 targeting studies, panitumumab or trastuzumab were, respectively, conjugated with ICG in the same manner as daclizumab. The number of ICG per antibody was 4 to 5 for the 1:10 reaction condition and 1 for the 1:1 reaction condition. Consequently, Dac-ICG(1:5), Pan-ICG(1:5), and Tra-ICG(1:5) were prepared under 1:5 antibody/ICG conditions, and Dac-ICG(1:1) and Tra-ICG(1:1) were prepared under 1:1 antibody/ICG conditions. Control human polyclonal IgG-Cy5.5 was synthesized in the similar manner as above using Cy5.5-NHS ester (GE Healthcare). The number of Cy5.5 per antibody was adjusted to 1.

Determination of quenching ability *in vitro*. For investigation of the quenching ability of bound ICG, all conjugates were treated with 5% SDS and 2-ME to diminish hydrophobic π-π interactions and separate IgG chains. The change in fluorescence intensity for each conjugate was investigated with an *in vivo* imaging system (Maestro, CRi, Inc.) using 710 to 760 nm excitation and 800 nm long-pass emission filters.

Cell culture. For IL-2Rα targeting studies, the IL-2Rα+ ATAC4 cell was used. As a negative control, the red fluorescent protein–transfected

Note: Supplementary data for this article are available at Cancer Research Online (http://cancerres.aacrjournals.org/).

Requests for reprints: Hisataka Kobayashi, Molecular Imaging Program, Center for Cancer Research/National Cancer Institute/NIH, Building 10, Room 1B40, Bethesda, MD 20892-1088. Phone: 301-451-4220; Fax: 301-402-3191; E-mail: kobayash@mail.nih.gov.

doi:10.1158/0008-5472.CAN-08-3116

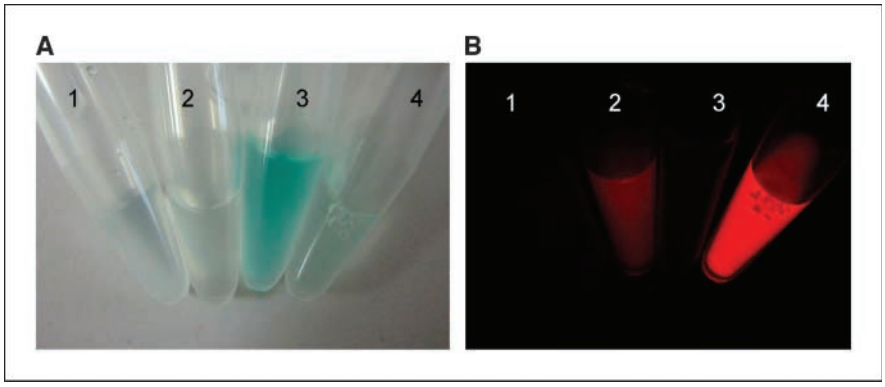

Figure 1. The bright field (*A*) and fluorescence (*B*) images of Ab-ICG conjugates. *1* and *2,* Zen-ICG(1:1); *3* and *4,* Zen-ICG(1:5). *1* and *3,* in PBS; *2* and *4,* SDS and 2-ME added condition. In PBS, all the conjugates have no fluorescence. The fluorescence was activated by treatment with SDS and 2-ME.

IL-2Rα− A431 cell (A431/DsRed) was used. For HER1 and HER2 targeting studies, HER1-positive A431 and MDA-MB468 cells and *HER2* gene–transfected NIH3T3 (3T3/HER2+) cell were used. Cell lines were grown in RPMI 1640 (Life Technologies) containing 10% fetal bovine serum (Life Technologies), 0.03% L-glutamine, 100 units/mL penicillin, and 100 μg/mL streptomycin in 5% CO_2 at 37°C.

Fluorescence microscopy studies. 3T3/HER2+ cells (1×10^4) were plated on a covered glass-bottomed culture well and incubated for 16 h. Then, Tra-ICG(1:1) or Tra-ICG(1:5) was added to the medium (30 μg/mL) and the cells were incubated for either 1 or 8 h. Cells were washed once with PBS, and fluorescence microscopy was performed using an Olympus BX61 microscope (Olympus America, Inc.) equipped with the following filters: excitation wavelength 672.5 to 747.5 nm, emission wavelength 765 to 855 nm. Transmitted light differential interference contrast images were also acquired.

Animal tumor model. All procedures were carried out in compliance with the Guide for the Care and Use of Laboratory Animal Resources (1996), National Research Council, and approved by the NIH Animal Care and Use Committee. For IL-2Rα targeting studies, ATAC4 cells (IL-2Rα+, 2×10^6) and A431/DsRed cells (IL-2Rα−, 2×10^6) were injected s.c. in the left and right dorsum of the mice, respectively. The experiments were performed 14 to 18 d after cell injection.

For HER1 and HER2 targeting studies, MDA-MB468 (HER1+, HER2−, 2×10^6 cells), A431 (HER1+, HER2−, 2×10^6 cells), and 3T3/HER2+ (HER1−, HER2+, 2×10^6 cells) were injected s.c. into the left flank, right buttock, and right flank, respectively.

***In vivo* CD25 targeted imaging studies.** Dac-ICG(1:1) or Dac-ICG(1:5) (50 μg) was injected via the tail vein into ATAC4 and A431/DsRed tumor-bearing mice. The mice were anesthetized with i.p. administered 10% sodium pentobarbital with 0.1% scopolamine butyl bromide; then, spectral fluorescence images were obtained with the Maestro (CRi) using two filter sets before and 1, 2, 3, and 4 d after injection. Two filter sets (green: excitation, 505–545 nm; emission, long-pass >563 nm and NIR: excitation, 710 to 760 nm; emission, long-pass >700 nm) were used to detect DsRed and ICG fluorescence. The spectral fluorescence images consisting of ICG, DsRed, and autofluorescence spectra were then unmixed based on their spectral patterns using commercial software (Maestro software, CRi). The regions of interest were placed on ICG spectrum images with reference to the white light and DsRed spectrum images to measure fluorescence intensities of ATAC4 and A431/DsRed tumors and body (background). After imaging at day 4, mice were sacrificed with carbon dioxide. Then, *ex vivo* imaging of the resected tumors was performed. Dissected lesions were embedded and stained with H&E.

***In vivo* tumor characterization study with HER1+ and HER2+ tumor-bearing mice.** Three tumor-bearing mice, two HER1+HER2− (MDA-MB468 and A431) and one HER2+HER1− (3T3/HER2+), were used. Pan-ICG(1:5) or Tra-ICG(1:5) (50 μg) was injected via tail vein and images were obtained 4 d after injection using the Maestro (CRi) with the ICG filter set. Histologic examination was performed with H&E staining.

***In vivo* two-color imaging with Pan-ICG or Tra-ICG compared with coinjected polyclonal human IgG-Cy5.5 to validate specificity of accumulation.** To validate the specific accumulation of Pan-ICG or

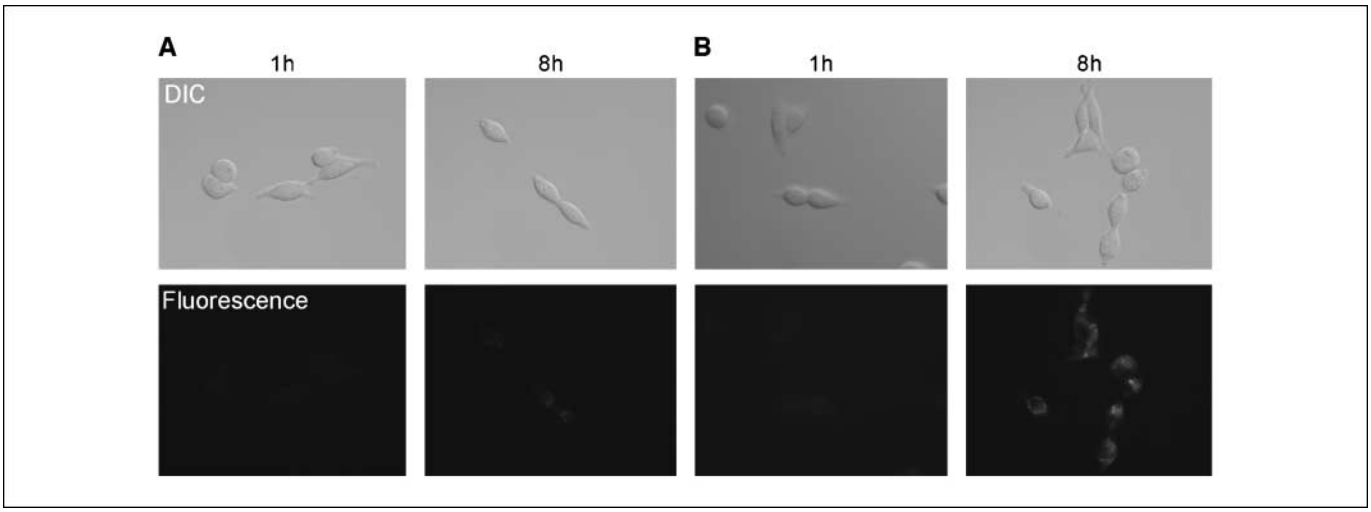

Figure 2. Fluorescence microscopy. 3T3/HER2+ cells were incubated with Tra-ICG(1:1) (*A*) or Tra-ICG(1:5) (*B*) for 1 or 8 h. The fluorescent signal on the cell surface was not observed after 1-h incubation. The fluorescent signal was detected after internalization into the cells by 8-h incubation. The signal was higher for Tra-ICG(1:5) than Tra-ICG(1:1). *DIC,* differential interference contrast.

Tra-ICG, control polyclonal human IgG-Cy5.5 was coinjected (50 μg, i.v.) with either Pan-ICG(1:5) or Tra-ICG(1:5) (50 μg, i.v.). *In vivo* and *ex vivo* spectral fluorescence images were obtained 4 d after injection into HER1+ and HER2+ tumor-bearing mice described above using Maestro. Two filter sets (red: excitation, 615–665 nm; emission, long-pass >700 nm and NIR: excitation, 710–760 nm; emission, long-pass >800 nm) separated Cy5.5 and ICG fluorescence. The fluorescence images consisting of spectra from ICG, Cy5.5, and autofluorescence were then unmixed with commercial software (Maestro software version 2.4, CRi) using the multiexcitation spectral analysis function. The dissected tumors were embedded in paraffin and stained with H&E.

Results

Antibody-fluorophore conjugates show high quenching capacity. The molecular interaction of ICG and mAb can be dissociated and disrupted with SDS and 2-ME treatments.

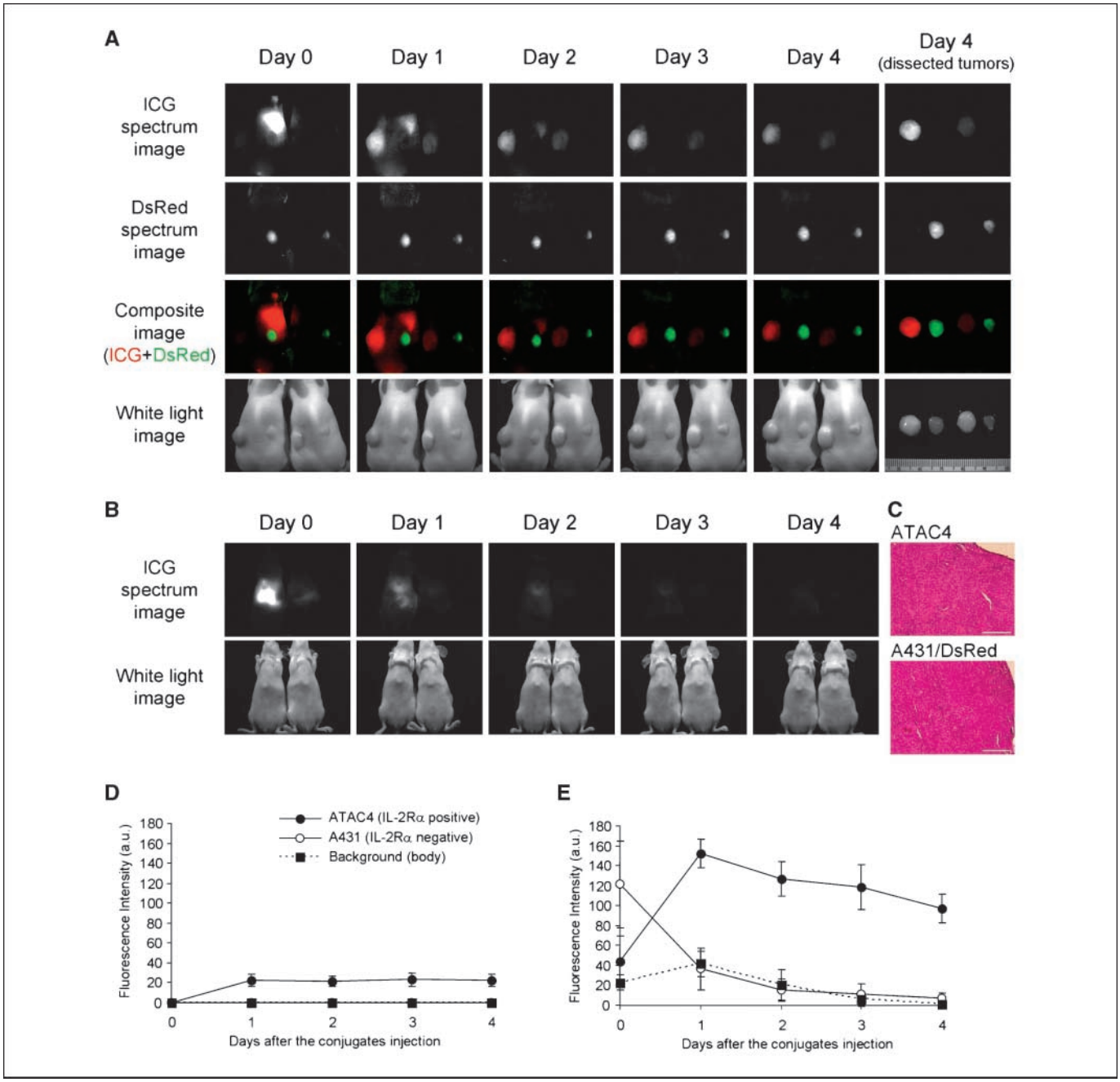

Figure 3. *In vivo* and *ex vivo* spectral fluorescence images with ATAC4 (*left dorsum*) and A431/DsRed (*right dorsum*) tumor-bearing mice (*A* and *B*). *A,* dorsal images. *B,* ventral images. Dac-ICG(1:5)–injected mouse is on the left side and Dac-ICG(1:1)–injected mouse is on the right side. The target tumor (ATAC4) was visualized by both conjugates, but the brightness was higher for Dac-ICG(1:5). The nontarget tumor (A431/DsRed) was not detected by either conjugate. *C,* H&E staining of dissected tumors (*bar,* 200 μm). Histologic findings of both tumors were identical. A high initial liver uptake was observed for Dac-ICG(1:5), but the clearance was rapid. The time course of ICG fluorescence intensities after i.v. injection of Dac-ICG(1:1) (*D*) or Dac-ICG(1:5) (*E*). The fluorescence intensity was increased only in the target tumor (ATAC4).

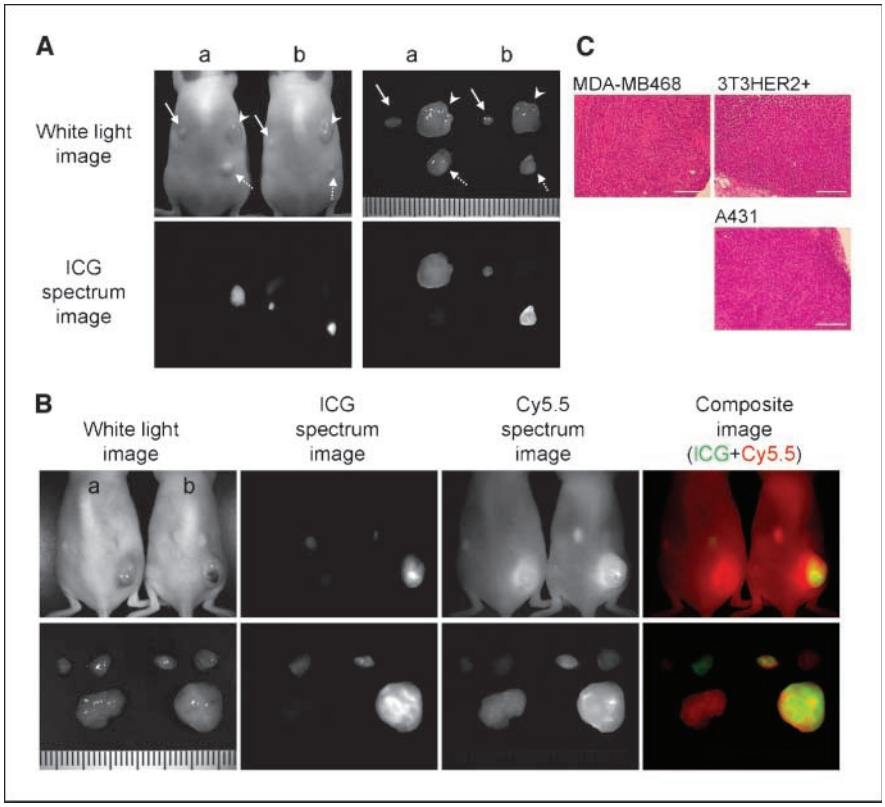

Figure 4. *A,* fluorescence imaging with HER1-positive and HER2-positive tumor-bearing mice. *Arrowhead,* 3T3/HER2 tumors (HER2-positive); *solid arrow,* MDA-MB468 tumors (HER1-positive); *dashed arrow,* A431 (HER1-positive) tumors. *a,* Tra-ICG(1:5)–injected mouse; *b,* Pan-ICG(1:5)–injected mouse. The images were obtained 4 d after the injection. Only the target-specific tumor was detected and tumor characterization was successful. *B,* human polyclonal human IgG-Cy5.5 was coinjected with Tra-ICG(1:5) (*a*) or Pan-ICG(1:5) (*b*) to validate specific accumulation. Only the target tumor was visualized with each specific ICG-conjugated antibody; however, all tumors were detected with IgG-Cy5.5. *C,* H&E staining of dissected tumors (*bar,* 200 μm).

Fluorescence intensity was low for all antibody-fluorophore conjugates before 5% SDS and 2-ME treatments; intense fluorescence was detected after dissociation (Fig. 1). The quenching capacities were 43, 6, 58, 44, and 10 for Dac-ICG(1:5), Dac-ICG(1:1), Pan-ICG(1:5), Tra-ICG(1:5), and Tra-ICG(1:1), respectively.

***In vitro* microscopic studies show fluorescence activation only within target HER2+ cells.** Fluorescence was not observed for either Tra-ICG(1:1) or Tra-ICG(1:5) inside the HER2+ cells after 1-h incubation; however, by 8 h, both conjugates showed fluorescence, which were brighter for Tra-ICG(1:5) than Tra-ICG(1:1) (Fig. 2). These results show that fluorescence activation occurs only after internalization within target cells, and minimal fluorescence is found outside the cell.

***In vivo* studies: target tumor was specifically visualized with ICG-conjugated daclizumab with high tumor-to-background ratio.** The time course fluorescence intensity in ATAC4 (IL2-Rα+) and A431/DsRed (IL2-Rα−) tumors after Dac-ICG(1:5) or Dac-ICG(1:1) is summarized in Fig. 3. The fluorescence increased only in target ATAC4 tumors and was higher for Dac-ICG(1:5) than Dac-ICG(1:1). The background and nontarget tumor fluorescence was low for both Dac-ICG(1:1) and Dac-ICG(1:5), whereas control human polyclonal IgG-Cy5.5 conjugate yielded similar fluorescence in both tumors (Supplementary Fig. S1). Histologic findings of both genetically modified A431 tumors were identical (Fig. 3*C*). The liver uptake was higher for Dac-ICG(1:5) (Fig. 3*B*). This high liver uptake affected the measured fluorescence intensity in A431/DsRed tumors just after Dac-ICG(1:5) injection (day 0), because tumors located near the liver. To check the cause of slight fluorescence from the body for Dac-ICG(1:5), blood fluorescence was measured 1 d after injection. However, the ICG signal was not detected in blood samples (Supplementary Fig. S2).

Tumors overexpressing cell surface receptors were successfully characterized *in vivo* using their respective ICG-conjugated antibodies. HER1+ tumors (MDA-MB468 and A431) were only visualized by Pan-ICG(1:5) and not by Tra-ICG(1:5). On the other hand, the HER2+ tumor (3T3/HER2+) was imaged only by Tra-ICG(1:5) (Fig. 4*A*). Coinjected control human polyclonal IgG conjugated with Cy5.5 resulted in similar fluorescence in all three tumors (Fig. 4*B*). Histologic findings of these three tumors showed expected differences in histology (Fig. 4*C*).

Discussion

A growing number of humanized mAbs directed against tumor-specific cell surface antigens have gained FDA approval and are successful in the clinic. If labeled with imaging "beacons," these mAbs could be used to diagnose and treat cancers. Such antibodies can be "labeled" with chelates that bind radioactive metals useful for diagnosis and therapy (11, 12). Radiolabeling, however, exposes patients to ionizing radiation and results in imaging with poor spatial and temporal resolution. Optical labeling overcomes these disadvantages but suffers from poor tissue penetration, preventing whole-body imaging. Among the fluorophores, NIR probes have the greatest tissue penetration and among the NIR probes only ICG is FDA approved for clinical use.

The use of ICG-conjugated antibodies has been limited because ICG loses its fluorescence once it is covalently bound to protein (8–10). Fluorescence, however, can be recovered from Ab-ICG conjugates by application of 5% SDS and 2-ME that release the ICG from the protein. Although the mechanism is still poorly understood, it is likely that a noncovalent interaction between the ICG and hydrophobic amino acids on IgG causes loss of fluorescence. Of course, this effect can be combined with classic

self-quenching to produce even higher quenching capacities. For instance, when the antibody to ICG ratio was increased to 1:5, quenching capacities of 43- to 58-fold were observed versus ~6-fold for the 1:1 conjugation. This property can be exploited *in vivo*. Trastuzumab binds to HER2 on the plasma membrane, and, subsequently, gradually internalized into the cytoplasm and then is delivered to lysosome to degenerate (13). It was observed in HER2+ cells that Tra-ICG became activated after 8 h of incubation, yielding virtually no signal before that. It is proposed that as Tra-ICG is internalized and cut into component peptides, releasing ICGs in the endosome-lysosome over 8 h. Similarly, uptake within tumors can be shown with matched Ab-ICG conjugates and antigen-expressing cell lines with minimal background signal. Thus, Ab-ICG conjugates are capable of labeling tumors *in vivo* with an FDA-approved NIR optical probe enabling tumors to be detected below the skin surface.

The Ab-ICG(1:5) conjugate releases weakly bound ICG or is partially trapped in the liver. ICG is catabolized in the liver and excreted into the bile, hence its use in assessing hepatic function in humans (14). Therefore, it is not surprising that considerable uptake in the liver 1 day after injection could be cleared quickly. This interfered with *in vivo* imaging by increasing scattered background signal especially for tumors placed near the liver. Fortunately, ICG is excreted relatively rapidly through the liver so that by day 3 liver signal was greatly reduced. The phenomenon of hepatic uptake was higher for the Ab:ICG(1:5) compounds; however, this was balanced by a much higher signal from the tumor itself.

Regarding clinical translation of Ab-ICG compounds, it is helpful that both mAbs (daclizimab, panitumumab, and trastuzumab) and the NIR fluorophore (ICG) are already FDA approved. Recognizing that conjugates may have different toxicities than their individual components, these agents will have to undergo extensive toxicity testing before human use; however, the presence of two approved agents in the conjugate certainly bodes well for its eventual clearance for human use compared with fluorescent proteins, which are excellent endogenous fluorescence emitters (15, 16), but require *in vivo* transfection that is unlikely to be permitted in humans in the near term (17).

Clinical translation of described agents will require detector/scanner systems for *in vivo* NIR fluorescence imaging in humans. NIR endoscopic cameras to assist surgery have been described (18, 19). In addition, a NIR clinical breast scanner has recently become available. Therefore, it is realistic to assume that this technology could be adapted for use with the ICG-mAb conjugates described here. Because the optical imaging system is simple and inexpensive compared with other imaging methods, it is likely that the method, if helpful in humans, would be readily accepted by clinicians.

Disclosure of Potential Conflicts of Interest

No potential conflicts of interest were disclosed.

Acknowledgments

Received 8/16/2008; revised 11/12/2008; accepted 11/17/2008; published OnlineFirst 01/27/2009.

Grant support: Intramural Research Program of the NIH, National Cancer Institute, Center for Cancer Research.

The costs of publication of this article were defrayed in part by the payment of page charges. This article must therefore be hereby marked *advertisement* in accordance with 18 U.S.C. Section 1734 solely to indicate this fact.

References

1. Sharma R, Wendt JA, Rasmussen JC, Adams KE, Marshall MV, Sevick-Muraca EM. New horizons for imaging lymphatic function. Ann N Y Acad Sci 2008;1131:13–36.
2. Weissleder R. A clearer vision for *in vivo* imaging. Nat Biotechnol 2001;19:316–7.
3. Sakka SG. Assessing liver function. Curr Opin Crit Care 2007;13:207–14.
4. Dzurinko VL, Gurwood AS, Price JR. Intravenous and indocyanine green angiography. Optometry 2004;75:743–55.
5. Urano Y, Asanuma D, Hama Y, et al. Selective molecular imaging of viable cancer cells with pH-activatable fluorescence probes. Nat Med 2009;15:104–9.
6. Kamiya M, Kobayashi H, Hama Y, et al. An enzymatically activated fluorescence probe for targeted tumor imaging. J Am Chem Soc 2007;129:3918–29.
7. Hama Y, Urano Y, Koyama Y, et al. A target cell-specific activatable fluorescence probe for *in vivo* molecular imaging of cancer based on a self-quenched avidin-rhodamine conjugate. Cancer Res 2007;67:2791–9.
8. Tadatsu Y, Muguruma N, Ito S, et al. Optimal labeling condition of antibodies available for immunofluorescence endoscopy. J Med Invest 2006;53:52–60.
9. Tadatsu M, Ito S, Muguruma N, et al. A new infrared fluorescent-labeling agent and labeled antibody for diagnosing microcancers. Bioorg Med Chem 2003;11:3289–94.
10. Muguruma N, Ito S, Hayashi S, et al. Antibodies labeled with fluorescence-agent excitable by infrared rays. J Gastroenterol 1998;33:467–71.
11. Waldmann TA. Immunotherapy: past, present and future. Nat Med 2003;9:269–77.
12. Goldenberg DM, Larson SM, Reisfeld RA, Schlom J. Targeting cancer with radiolabeled antibodies. Immunol Today 1995;16:261–4.
13. Harari D, Yarden Y. Molecular mechanisms underlying ErbB2/HER2 action in breast cancer. Oncogene 2000;19:6102–14.
14. Cherrick GR, Stein SW, Leevy CM, Davidson CS. Indocyanine green: observations on its physical properties, plasma decay, and hepatic extraction. J Clin Invest 1960;39:592–600.
15. Hoffman RM. The multiple uses of fluorescent proteins to visualize cancer *in vivo*. Nat Rev Cancer 2005;5:796–806.
16. Hasegawa S, Yang M, Chishima T, et al. *In vivo* tumor delivery of the green fluorescent protein gene to report future occurrence of metastasis. Cancer Gene Ther 2000;7:1336–40.
17. Yang M, Baranov E, Moossa AR, Penman S, Hoffman RM. Visualizing gene expression by whole-body fluorescence imaging. Proc Natl Acad Sci U S A 2000;97:12278–82.
18. Upadhyay R, Sheth RA, Weissleder R, Mahmood U. Quantitative real-time catheter-based fluorescence molecular imaging in mice. Radiology 2007;245:523–31.
19. Tanaka E, Choi HS, Fujii H, Bawendi MG, Frangioni JV. Image-guided oncologic surgery using invisible light: completed pre-clinical development for sentinel lymph node mapping. Ann Surg Oncol 2006;13:1671–81.